



Quarterly peer-reviewed scientific journal

ISSN 1505-4675
e-ISSN 2083-4527

TECHNICAL SCIENCES

Homepage: www.uwm.edu.pl/techsci/



UNSTEADY HYDROMAGNETIC FLOW OF OLDROYD-B FLUID OVER AN OSCILLATORY STRETCHING SURFACE: A MATHEMATICAL MODEL

*Sami Ullah Khan*¹, *Nasir Ali*²

¹ Department of Mathematics, Comsats Institute of Information Technology, Pakistan

² Department of Mathematics and Statistics, International Islamic University, Pakistan

Received 16 April 2016, accepted 27 January 2017, available online 30 January 2017.

Key words: Oldroyd-B fluid, oscillatory stretching sheet, homotopy analysis method.

Abstract

In the present work, we have studied an unsteady, two-dimensional boundary layer flow of a magnetohydrodynamics (MHD) Oldroyd-B fluid over an oscillatory stretching surface. The problem is modeled by using constitutive equations. The number of independent variables in the governing equations are reduced by using appropriate dimensionless variables. The analytical solution is computed by using homotopy analysis method. The influences of various physical parameters such as Deborah numbers, ratio of angular frequency to stretching rate parameter and Hartmann number on time-series of velocity and transverse velocity profiles at different time instants are investigated and discussed quantitatively with the help of various graphs. It is observed that amplitude of velocity increases by increasing ratio of oscillating frequency to stretching rate parameter while decreases by increasing Hartmann number. It is further observed that the magnitude of velocity decreases by increasing Hartmann number and Deborah numbers in the terms of relaxation time parameter.

Introduction

The analysis of boundary layer flow caused by moving stretching surface has promising applications in many industrial and technological processes. These applications include metal spinning, metal extrusion, glass blowing, artificial fibers, filaments and wires and many more. Several authors have investigated the boundary layer flow of viscous fluids over stretching surfaces.

Correspondence: Sami Ullah Khan, Department of Mathematics, Comsats Institute of Information Technology, Sahiwal 57000, Pakistan, e-mail: sk_iiu@yahoo.com

CRANE (1970) computed an exact analytic solution of a viscous fluid over a linearly stretching surface. POP et al. (1996) investigated the unsteady boundary layer flow of viscous fluid over stretching surface. VARSHNEY (1979) discussed the fluctuating flow of viscous fluid over a saturated porous plate. WANG (1988) analyzed the boundary layer flow of viscous fluid over an oscillatory stretching surface by using perturbation technique. MUKHOPADHYAY et al. (2013) computed numerical solution of boundary layer flow of a Maxwell fluid over a stretching permeable surface in the presence of thermal radiation. ABBAS et al. (2009) discussed the two-dimensional boundary layer flow of a viscous fluid over an oscillatory stretching surface. ELSHEHAWAY et al. (2003) studied the effects of inclined magnetic field on the magneto fluid flow through a porous medium between two inclined wavy porous plates.

The study of hydromagnetic flow has engaged the attention of scientists and engineering due to its promising applications in the hydrodynamic processes and in the field of chemistry, physics, polymer industry and metallurgy. The electrically conducting fluid under the influence of magnetic field has prime importance in the cooling process to control the rate of cooling. Having such salient features in mind, many authors studied the MHD flows in different flow configurations (HAYAT et al. 2015, RAJU et al. 2015, ABBAS 2008).

In past few years, the study of non-Newtonian fluids has received much attention of engineers and scientists because of their practical applications in chemical and nuclear industries, polymer solutions, bioengineering engineering etc. It is well established fact that nonlinear fluids obey nonlinear relationship between shear stress and rate of deformation. Among these nonlinear fluids, Oldroyd-B fluid is the class of fluids that attracted the attentions of researchers in recent times. Oldroyd-B fluid model is one of the models which exhibit the relaxation and retardation time effects. The literature survey shows that much attention is given on steady flow of Oldroyd-B fluid over a stretching sheet. We highlight some of them. RAJAGOPAL and BHATNAGAR (1995) studied the flow of an Oldroyd-B fluid over an infinite porous plate by computing asymptotically decaying solution. SAJID et al. (2010) presented the numerical solution for two-dimensional boundary flow of an incompressible Oldroyd-B fluid over a stretching surface. Later on, HAYAT et al. (2014) investigated the three dimensional flow and heat transfer of an Oldroyd-B fluid over a bidirectional stretching surface. In another paper, HAYAT et al. (2015) used homotopy analysis method to discuss the mixed convection flow of an Oldroyd-B fluid in a doubly stratified surface. ZHENG et al. (2011) computed exact solution of generalized Oldroyd-B over accelerating infinite plate.

In all above mentioned studies, the authors studied the steady flow of Oldroyd-B fluid in the given geometries. The aim of present work is to

investigate an unsteady boundary layer flow of an Oldroyd-B fluid in presence of uniform magnetic field. The flow is induced by an oscillatory stretching sheet which stretched and oscillates periodically in its own plane. The consideration unsteady flow of Oldroyd-B fluid and magnetic field effects makes the study quite versatile and general. The results of important studies carried out previously (WANG 1988, ABBAS et al. 2008, HAYAT et al. 2010, TURKYILMAZOGLU 2013, ZHENG et al. 2013, ALI 2015, SHEIKH, ABBAS 2015, ALI et al. 2016) and can be found from this study. The dimensionless partial differential equations are solved analytically by using well known homotopy analysis method (LIAO 2004, ABBASBANDY 2007, TURKYILMAZOGLU 2009, 2012). Graphical results illustrating the behavior of velocity is shown and discussed in detail.

Mathematical Model

The flow analysis is based on the following laws.

Law of conservation of mass:

$$\operatorname{div}\mathbf{V} = 0 \quad (1)$$

Law of conservation of momentum:

$$\rho \frac{d\mathbf{V}}{dt} = \operatorname{div}\mathbf{T} + \mathbf{J} \cdot \mathbf{B} \quad (2)$$

where \mathbf{V} is the velocity vector, \mathbf{J} is the current density, \mathbf{B} is the magnetic flux vector, ρ is the density of the fluid, \mathbf{T} is the Cauchy stress tensor, d/dt represents the material derivative. We define Cauchy stress tensor

$$\mathbf{T} = -p\mathbf{I} + \mathbf{S} \quad (3)$$

where \mathbf{S} is the extra stress tensor which satisfies the following relation (HAYAT 2015):

$$\mathbf{S} + \lambda_1 \frac{D\mathbf{S}}{Dt} = \mu \left(\mathbf{A} + \lambda_2 \frac{D\mathbf{A}}{Dt} \right) \quad (4)$$

where

$$\frac{D\mathbf{S}}{Dt} = \frac{d\mathbf{S}}{dt} - \mathbf{S}\mathbf{L} - \mathbf{L}^*\mathbf{S}, \text{ for a second order tensor} \quad (5)$$

In above equations λ_1 is the relaxation time, λ_2 is the retardation time, μ is the dynamic viscosity, $*$ denotes the matrix transpose and \mathbf{A}_1 is the first Rivlin-Ericksen tensor which is defined as

$$\mathbf{A}_1 = \nabla \mathbf{V} + \nabla \mathbf{V}^* \quad (6)$$

The current density \mathbf{J} appeared in Eq. (2) is defined as

$$\mathbf{J} = \sigma (\mathbf{V} \cdot \mathbf{B}) \quad (7)$$

in which σ is the electrical conductivity.

Flow Analysis

We consider a two-dimensional and incompressible flow of electrically conducting Oldroyd-B fluid over an oscillatory stretching surface (at $\bar{y} = 0$) and fluid occupy the space $\bar{y} > 0$. We choose a cartesian coordinate system (\bar{x}, \bar{y}) . It is assumed that the sheet is stretched with velocity $u_w = b\bar{x} \sin \omega t$ (b is the stretching rate and ω is the angular frequency) in \bar{x} - direction under the action of two equal and opposite forces. Further, external magnetic field of constant magnitude B_0 is imposed in \bar{y} direction and effects of induced magnetic field are neglected under the assumption of very large magnetic diffusivity.

For flow under consideration, the appropriate velocity field is

$$\mathbf{V} = [u(\bar{x}, \bar{y}, t), v(\bar{x}, \bar{y}, t), 0] \quad (8)$$

where u and v represents the velocity components along \bar{x} and \bar{y} directions, respectively. Inserting Eq. (8) in Eqs. (1)–(7) and employing boundary layer approximations, we get the following equations

$$\frac{\partial u}{\partial \bar{x}} + \frac{\partial v}{\partial \bar{y}} = 0 \quad (9)$$

$$\begin{aligned} \frac{\partial u}{\partial t} + u \frac{\partial u}{\partial \bar{x}} + v \frac{\partial u}{\partial \bar{y}} + \lambda_1 \left(\frac{\partial^2 u}{\partial t^2} + 2u \frac{\partial^2 u}{\partial t \partial \bar{x}} + 2v \frac{\partial^2 u}{\partial t \partial \bar{y}} + u^2 \frac{\partial^2 u}{\partial \bar{x}^2} + v^2 \frac{\partial^2 u}{\partial \bar{y}^2} + 2uv \frac{\partial^2 u}{\partial \bar{x} \partial \bar{y}} \right) = \\ v \frac{\partial^2 u}{\partial \bar{y}^2} + v \lambda_2 \left(\frac{\partial^3 u}{\partial t \partial \bar{y}^2} + u \frac{\partial^3 u}{\partial \bar{x} \partial \bar{y}^2} + v \frac{\partial^3 u}{\partial \bar{y}^3} - \frac{\partial u}{\partial \bar{x}} \frac{\partial^2 u}{\partial \bar{y}^2} - \frac{\partial u}{\partial \bar{y}} \frac{\partial^2 v}{\partial \bar{y}^2} \right) - \frac{\sigma B_0^2}{\rho} \left(u + \lambda_1 \frac{\partial u}{\partial t} + v \lambda_1 \frac{\partial u}{\partial \bar{y}} \right) \end{aligned} \quad (10)$$

where ν represents the kinematic viscosity. Eq. (10) is subjected to the following boundary conditions

$$u = u_\omega = b\bar{x} \sin \omega t, v = 0, \text{ at } \bar{y} = 0, t > 0 \quad (11)$$

$$u \rightarrow 0, \frac{\partial u}{\partial \bar{y}} \rightarrow 0 \text{ as } \bar{y} \rightarrow \infty \quad (12)$$

We introduce following dimensionless variables (WANG 1988)

$$y = \sqrt{\frac{b}{\nu}} \bar{y}, \quad \tau = t\omega, \quad u = b\bar{x}f_y(y, \tau), \quad v = -\sqrt{\nu b} f(y, \tau) \quad (13)$$

The continuity Eq. (9) is identically satisfied and Eq. (10) reduces to

$$\begin{aligned} f_{yyy} + (1 + M\beta_1) ff_{yy} - S(1 + \beta_1 M) f_{y\tau} - Mf_y - f_y^2 \\ -\beta_1(S^2 f_{y\tau\tau} + 2S(f_y f_{y\tau} - ff_{yy\tau}) + f^2 f_{yyy} - 2ff_y f_{yy}) + \beta_2(Sf_{yyy\tau} + f_{yy}^2 - ff_{yyyy}) = 0 \end{aligned} \quad (14)$$

The boundary conditions in dimensionless form are

$$f_y(0, \tau) = \sin \tau, f(0, \tau) = 0 \quad (15)$$

$$f_y(\infty, \tau) \rightarrow 0, f_{yy}(\infty, \tau) \rightarrow 0 \quad (16)$$

where $\beta_1 = \lambda_1 b$ and $\beta_2 = \lambda_2 b$ are the dimensionless Deborah numbers in the terms of relaxation and retardation times, respectively, $S = \omega/b$ is the ratio of oscillating frequency to stretching rate parameter and $M = \sqrt{\sigma B_0^2 / \rho b}$ is the Hartmann number.

Series solution by homotopy analysis method

To start our simulation via the homotopy analysis method, we suggest the following initial guess for velocity profile

$$f_0(y, \tau) = \sin \tau(1 - \exp(-y)) \quad (17)$$

with linear operator

$$\mathcal{L}_f = \frac{\partial^3}{\partial y^3} - \frac{\partial}{\partial y} \tag{18}$$

with property

$$\mathcal{L}_f[C_1 + C_2 \exp(y) + C_3 \exp(-y)] = 0 \tag{19}$$

where C_i ($i = 1,2,3$) are arbitrary constants.

Zeroth-order deformation problems

The zeroth-order deformation for given problem is constructed as

$$(1 - p) \mathcal{L}_f [\hat{f}(y, \tau, p) - f_0(y, \tau)] = ph_f N_f [\hat{f}(y, \tau, p)] \tag{20}$$

$$\hat{f}(0, \tau, p) = 0, \left. \frac{\partial \hat{f}(y, \tau, p)}{\partial y} \right|_{y=0} = \sin \tau, \left. \frac{\partial \hat{f}(y, \tau, p)}{\partial y} \right|_{y=0} = 0, \left. \frac{\partial^2 \hat{f}(y, \tau, p)}{\partial y^2} \right|_{y=\infty} = 0 \tag{21}$$

where $p \in [0,1]$ is an embedding parameter. The associated nonlinear operator N_f is

$$\begin{aligned} N_f [\hat{f}(y, \tau, p)] &= \frac{\partial^3 \hat{f}(y, \tau, p)}{\partial y^3} - S(1 + \beta_1 M) \frac{\partial^2 \hat{f}(y, \tau, p)}{\partial y \partial \tau} + \\ &+ S(1 + \beta_1 M) \hat{f}(y, \tau, p) \frac{\partial^2 \hat{f}(y, \tau, p)}{\partial y^2} \\ &- M \frac{\partial \hat{f}(y, \tau, p)}{\partial y} - \left(\frac{\partial \hat{f}(y, \tau, p)}{\partial y} \right)^2 \end{aligned} \tag{22}$$

$$\begin{aligned} -\beta_1 &\left(S^2 \frac{\partial^3 \hat{f}(y, \tau, p)}{\partial \tau^2 \partial y} + 2S \left(\frac{\partial \hat{f}(y, \tau, p)}{\partial y} \frac{\partial^2 \hat{f}(y, \tau, p)}{\partial y \partial \tau} - f \frac{\partial^3 \hat{f}(y, \tau, p)}{\partial y^2 \partial \tau} \right) \right) \\ &+ \hat{f}^2(y, \tau, p) \frac{\partial^3 \hat{f}(y, \tau, p)}{\partial y^3} - 2 \hat{f}(y, \tau, p) \frac{\partial \hat{f}(y, \tau, p)}{\partial y} \frac{\partial^2 \hat{f}(y, \tau, p)}{\partial y} \\ &+ \beta_2 \left(S \frac{\partial^4 \hat{f}(y, \tau, p)}{\partial y^3 \partial \tau} + \left(\frac{\partial^2 \hat{f}(y, \tau, p)}{\partial y^2} \right)^2 - \hat{f}(y, \tau, p) \frac{\partial^4 \hat{f}(y, \tau, p)}{\partial y^4} \right) \end{aligned}$$

The zeroth-order deformation problems defined above have the following solutions corresponding to $p = 0$ and $p = 1$

$$\hat{f}(y, \tau, 0) = f_0(y, \tau), \hat{f}(y, \tau, 1) = f(y, \tau) \tag{23}$$

Using Taylor’s series expansion, we can write

$$\hat{f}(y, \tau, p) = f_0(y, \tau) + \sum_{m=1}^{\infty} f_m(y, \tau) = \frac{1}{m!} \left. \frac{\partial^m \hat{f}(y, \tau, p)}{\partial p^m} \right|_{p=0} \tag{24}$$

The convergence of above series solution depends upon h_f . We assume that h_f is selected so that Eq. (24) converges at $p = 1$. Therefore

$$f(y, \tau) = f_0(y, \tau) + \sum_{m=1}^{\infty} f_m(y, \tau) \tag{25}$$

***m*th-order deformation problems**

$$\mathcal{L}_f [f_m(y, \tau) - \chi_m f_{m-1}(y, \tau)] = h_f R_m^f(y, \tau) \tag{26}$$

$$f_m(0, \tau) = 0, \frac{\partial f_m(0, \tau)}{\partial y} = 0, \frac{\partial f_m(\infty, \tau)}{\partial y} = 0, \frac{\partial^2 f_m(\infty, \tau)}{\partial y^2} = 0 \tag{27}$$

$$\begin{aligned} R_m^f(y, \tau) = & \frac{\partial f_{m-1}}{\partial y^3} - S(1 + M\beta_1) \frac{\partial^2 f_{m-1}}{\partial y \partial \tau} - M \frac{\partial f_{m-1}}{\partial y} + (1 + M\beta_1) \sum_{k=0}^{m-1} \left(f_{m-1-k} \frac{\partial^2 f_k}{\partial y^2} \right) \\ & - \beta_1 S^2 \frac{\partial^3 f_{m-1}}{\partial y \partial \tau^2} + \beta_2 S \frac{\partial^4 f_{m-1}}{\partial y^3 \partial \tau} - 2S\beta_1 \sum_{k=0}^{m-1} \left(\frac{\partial f_{m-1-k}}{\partial y} \frac{\partial^2 f_k}{\partial y \partial \tau} - f_{m-1-k} \frac{\partial^3 f_k}{\partial y^2 \partial \tau} \right) \\ & - \beta_1 \sum_{k=0}^{m-1} f_{m-1-k} \sum_{l=0}^{m-1} f_{k-1} \frac{\partial^3 f_l}{\partial y^3} + 2\beta_1 \sum_{k=0}^{m-1} f_{m-1-k} \sum_{l=0}^{m-1} \frac{\partial f_{k-l}}{\partial y} \frac{\partial^2 f_l}{\partial y^2} + \beta_2 \sum_{m=0}^{m-1} \frac{\partial f_{m-l-k}}{\partial y^2} \frac{\partial^2 f_k}{\partial y^2} \\ & - \beta_2 \sum_{k=0}^{m-1} f_{m-1-k} \frac{\partial^4 f_k}{\partial y^4} \end{aligned} \tag{28}$$

Here χ_m is defined as

$$\chi_m = \begin{cases} 0, & m \leq 1, \\ 1, & m > 1. \end{cases}$$

The general solution at m th-order deformation Eq. (26) can be defined as

$$f_m(y, \tau) = f_m^*(y, \tau) + C_1 + C_2 \exp(y) + C_3 \exp(-y) \quad (29)$$

where $f_m^*(y, \tau)$ represent the special solution.

Convergence of HAM Solution

The proper choice of the auxiliary parameters h_f is important for convergence of the HAM solution. For a particular set of parameters, the convergence region can be obtained by plotting the so-called h -curves. Figure 1 presents the regions for plausible values of h_f for a given set of parameter. From figure, it is clear that convergent solution can be obtained when $-1.5 \leq h_f \leq 0$. Tables 1 and 2 show a comparison of numerical values of $f_m^*(0, \tau)$ with the already reported values in refs. TURKYILMAZOGLU (2013), HAYAT et al. (2010), ZHENG et al. (2013), ABBAS et al. (2008). It is observed that our results are in excellent agreement with the already available results. This testifies the validity of our solution and the graphical results presented in the subsequent section.

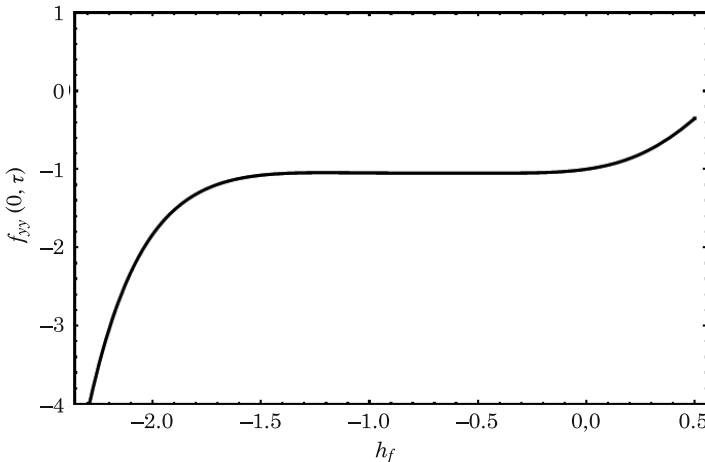


Fig. 1. h -curve for velocity profile at 8th order of approximation with $M = 0.1, S = 0.2, \beta_1, \beta_2 = 0.1, \tau = 0.5\pi$

Table 1

A comparison of values of $f^*(0, \tau)$ with the existing ones reported in Refs ZHENG et al. (2013), ABBAS et al. (2008)

S	M	τ	ZHENG et al. (2013)	ABBAS et al. (2008)	Present results $\beta_1 = \beta_2 = 0$
1.0	12	1.5π	11.678565	11.678656	11.678565
		5.5π	11.678706	11.678707	11.678706
		9.5π	11.678656	11.678656	11.678656

Table 2

A comparison of values of $f^*(0, \tau)$ for different values of M with the existing ones reported in Refs TURKYILMAZOGLU (2013), HAYAT (2010)

M	HAYAT (2010)	TURKYILMAZOGLU (2013)	Present results $\beta_1 = \beta_2 = S = 0, \tau = \pi / 2$
0	- 1.000000	-1.00000000	-1.000000
0.5	-1.224747	-1.22474487	-1.224747
1.0	-1.414217	-1.41421356	-1.414217
1.5	-1.581147	-1.58113883	-1.581147
2.0	-1.732057	-1.73205081	-1.732057

Results and discussion

The analytical procedure explained in the previous section is adopted for the solution of the Eq. (14) with boundary conditions (15) and (16). The aim of this section is to present the graphical results and their interpretation. For this purpose, the effects of various parameters like Deborah numbers β_1 and β_2 ratio of angular frequency to stretching rate S and Hartmann number M on velocity profile are shown graphically.

Figure 2a-d presents the effects of Deborah numbers (β_1, β_2), Hartmann number M and ratio of angular frequency to stretching rate S on time-series of the velocity profile f' . The effects of Deborah number β_1 on the time-series of velocity profile f' is shown in Figure 2a. It is observed that the amplitude of the velocity decreases with increasing Deborah number β_1 . It is due to the fact that β_2 contains relaxation time which provides the resistance to the flow due to viscoelastic properties of the fluid. The variation of the time-series of the velocity profile with time τ for various values of β_2 is presented in Figure 2b. As expected, opposite behavior is observed as compared with Figure 2a i.e., the velocity decreases with increasing β_2 . Figure 2c illustrates the effects of ratio of angular frequency to stretching rate S on the time-series of the velocity by keeping $M = 0.5, \beta_1 = 1, \beta_2 = 0.5$. It is observed that an increase in

S results in a pronounced phase shift and rise in the amplitude of oscillations. Figure 2d displays the effects of Hartmann number on time-series of velocity profile. It is observed that the amplitude of velocity decreases with increasing Hartmann number. Such effects are expected because the fact that magnetic force produces a Lorentz force which act as resistance to amplitude of flow velocity.

Figure 3a, b displays the effect of Deborah number β_1 on the transverse profile of the velocity at two different time instants $\tau = 8.5\pi$ and $\tau = 9.5\pi$. Figure 2a reveals that at time instant $\tau = 8.5\pi$ the velocity decreases from unity to zero inside the boundary layer. The suppression of amplitude is a direct consequence of the elastic nature of fluid. Moreover, an increase in β_1 results in decrease in the momentum boundary layer thickness. Figure 3b shows the influence of β_1 at time instant $\tau = 9.5\pi$. Due to increase in β_1 the velocity of the fluid decreases and ultimately decreases the momentum boundary layer thickness.

The variation of transverse profile of velocity for various values of β_2 at two different time instants $\tau = 8.5\pi$ and $\tau = 9.5\pi$ is shown in Figure 4a, b. The transverse profiles of velocity illustrating the effects of β_2 at time instant $\tau = 8.5\pi$ are plotted in Figure 4a. It is observed that the magnitude of the velocity increases by increases β_2 . It can be justified physically as β_2 is associated with retardation time which increases with increase of β_2 . This increase in retardation time is responsible to increase the velocity of the fluid. Similarly at time instant $\tau = 9.5\pi$ the velocity increases from at the wall to zero far away from the surface. The momentum boundary layer thickness also increases at this time instant.

Figure 5a and b demonstrates the effect of Hartmann number on the velocity profile at $\tau = 8.5\pi$ and $\tau = 9.5\pi$, respectively. It is found that an increase in the Hartmann number M results in decrease in the velocity profile at both time instants. In fact the application of magnetic force produces a resistive force known as Lorentz force which has tendency to oppose the amplitude of the velocity. The effects of ratio of oscillating frequency to stretching rate parameter S on transverse profile of velocity at two different time instants $\tau = 8.5\pi$ and $\tau = 9.5\pi$ are shown in Figure 6a and b. From Figure 6a, it is clear at time instant $\tau = 8.5\pi$ the velocity profile increases with increasing ratio of oscillating frequency to stretching rate parameter S . The momentum boundary layer thickness also increases with increasing S . In contrast, Figure 6b shows a decrease in the amplitude of flow velocity with the ratio of oscillating frequency to stretching rate parameter S at time instant $\tau = 9.5\pi$.

Concluding remarks

We have investigated an unsteady two-dimensional boundary layer flow of Oldroyd-B fluid over an oscillatory stretching sheet by using boundary layer approximations. A well known analytic technique namely homotopy analysis method is used to compute the series solution. Study reveals that the time-series of amplitude of the velocity increases by increasing ratio of angular frequency to stretching parameter S and retardation time parameter β_2 , The effects of material parameters β_1 and β_2 on the velocity profile are quite opposite. It is also observed that the amplitude of velocity decreases by increasing Hartmann number.

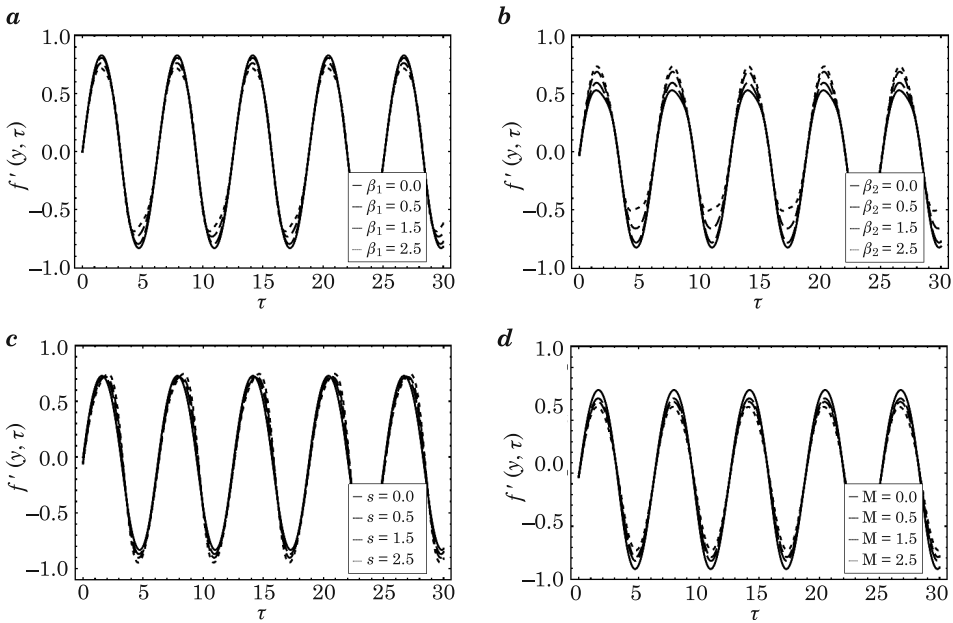


Fig. 2. Time-series of velocity profile for different values of: a - β_1 with $S = 0.2$, $M = 0.2$, $\beta_1 = 1.5$, b - β_2 with $M = 1.5$, $S = 0.1$, $\beta_1 = 2.6$, c - S with $M = 0.5$, $\beta_1 = 1$, $\beta_2 = 0.5$, d - M with $S = 0.5$, $\beta_1 = 1$, $\beta_2 = 0.5$

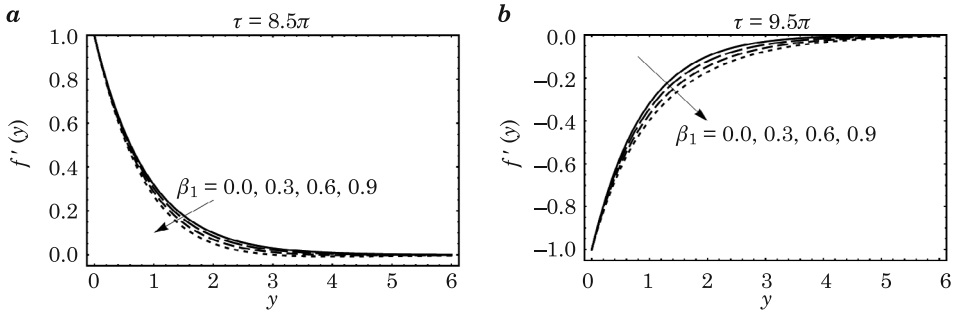


Fig. 3. Velocity profile for different values of β_1 with $M = 2, S = 0.7, \beta_2 = 0.5$

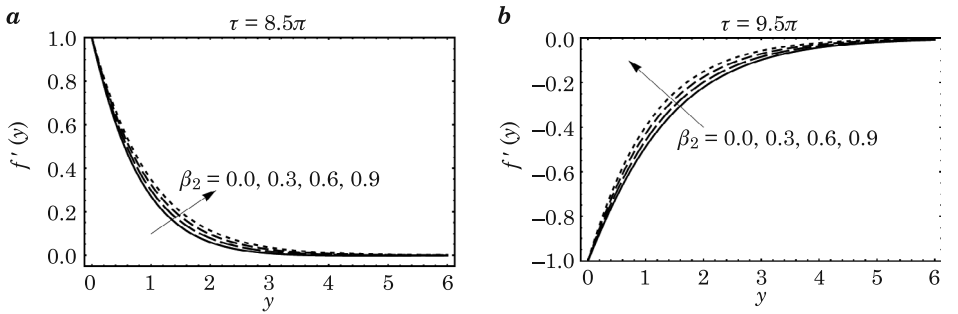


Fig. 4. Velocity profile for different values of β_2 with $M = 0.2, S = 0.1, \beta_1 = 1$

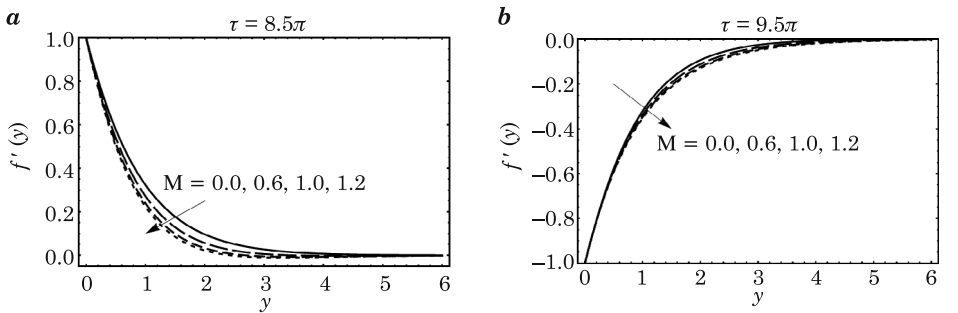


Fig. 5. Velocity profile for different values of M with $S = 0.1, \beta_1 = 3, \beta_2 = 1$

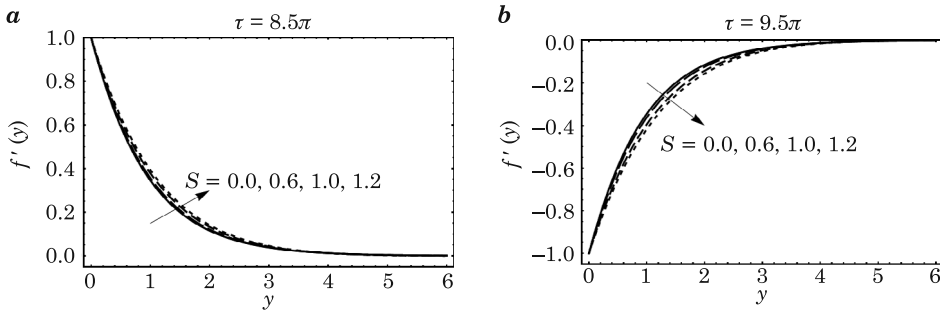


Fig. 6. Velocity profile for different values of S with $M = 0.1$, $\beta_1 = 3$, $\beta_2 = 1$

Acknowledgments

We are thankful to the anonymous reviewer for his/her useful comments to improve the earlier version of the paper.

References

- ABBAS Z., WANG Y., HAYAT T., OBERLACK M. 2008. *Hydromagnetic flow in a viscoelastic fluid due to the oscillatory stretching surface*. *Int. J. Nonlinear Mech.*, 43(8): 783–797, <http://dx.doi.org/10.1016/j.ijnonlinmec.2008.04.009>.
- ABBAS Z., WANG Y., HAYAT T., OBERLACK M. 2009. *Slip effects and heat transfer analysis in a viscous fluid over an oscillatory stretching surface*. *Int. J. Numer. Meth. Fluids*, 59: 443–458.
- ABBASBANDY S. 2007. *Homotopy Analysis Method for Heat Radiation Equations*. *Int. Commun. Heat Mass Transfer*, 34: 380–387.
- ALI N., KHAN S.U., ABBAS Z. 2015. *Hydromagnetic Flow and Heat Transfer of a Jeffrey Fluid over an Oscillatory Stretching Surface*. *Z. Naturforsch., A*, 70(7): 567–576.
- ALI N., KHAN S.U., ABBAS Z., SAJJID M. 2016. *Soret and Dufour effects on hydromagnetic flow of viscoelastic fluid over porous oscillatory stretching sheet with thermal radiation*. *J. Braz. Soc. Mech. Sci. Eng.*, 38: 2533–2546.
- CRANE L.J. 1970. *Flow past a stretching plate*. *Z. Angew. Math. Phys. (ZAMP)*, 21: 645–647.
- ELSHEHAWY E.F., ELSAYED M.E., ELBARBARY N.E. 2003. *Effect of inclined magnetic field on magneto fluid flow through a porous medium between two inclined wavy porous plates (numerical study)*. *Applied Mathematics and Computation*, 135(1): 85–103.
- HAYAT T., MUHAMMAD T., SHEHZAD S.A., ALSAEDI A. 2015a. *Temperature and Concentration Stratification Effects in Mixed Convection Flow of an Oldroyd-B Fluid with Thermal Radiation and Chemical Reaction*. *PLoS ONE* 10(6): e0127646, doi: 10.1371/journal.pone.0127646.
- HAYAT T., MUSTAFA M., POP I. 2010. *Heat and mass transfer for Soret and Dufour's effect on mixed convection boundary layer flow over a stretching vertical surface in a porous medium filled with a viscoelastic fluid*. *Commun. Nonlinear Sci. Numer. Simul.*, 15: 1183–1196.
- HAYAT T., SHAFIQ A., ALSAEDI A., ASGHAR S. 2015b. *Effect of inclined magnetic field in flow of third grade fluid with variable thermal conductivity*. *AIP Advances*, 5: 087108, doi: <http://dx.doi.org/10.1063/1.4928321>.
- HAYAT T., SHEHZAD S.A., MEZEL S.A., ALSAEDI A. 2014. *Three-dimensional flow of an Oldroyd-B fluid over a bidirectional stretching surface with prescribed surface temperature and prescribed surface heat flux*. *J. Hydrol. Hydromech.*, 62: 117–125.

- LIAO S.J. 2004. *On the homotopy analysis method for nonlinear problems*. App. Mathematics and Computation, 147: 499–513.
- MUKHOPADHYAY S., RANJAN DE P., LAYEK G.C. 2013. *Heat transfer, characteristics for the Maxwell fluid flow past an unsteady stretching permeable surface embedded in a porous medium with thermal radiation*. Journal of Applied Mechanics and Technical Physics, 54(3): 385–396.
- POP I., NA T.Y. 1996. *Unsteady flow past a stretching sheet*. Mechanics Research Communications, 23: 413–422.
- RAJAGOPAL K.R., BHATNAGAR R.K. 1995. *Exact solutions for some simple flows of an Oldroyd-B fluid*. Acta Mechanica, 113: 233–239.
- RAJU C.S.K., SANDEEP N., SULOCHANA C., SUGUNAMMA V., JAYACHANDRA BABU M. 2015. *Radiation, inclined magnetic field and cross-diffusion effects on flow over a stretching surface*. Journal of the Nigerian Mathematical Society, 34: 169–180.
- SAJID M., ABBAS Z., JAVED T., ALI N. 2010. *Boundary layer flow of an Oldroyd-B fluid in the region of stagnation point over a stretching sheet*. Canadian Journal of Physics, 88: 635–640.
- SHEIKH M., ABBAS Z. 2015. *Effects of thermophoresis and heat generation/absorption on MHD flow due to an oscillatory stretching sheet with chemically reactive species*. Journal of Magnetism and Magnetic Materials, S0304-8853(15): 3043.
- TURKYILMAZOGLU M. 2009. *Purely Analytic Solutions of the Compressible Boundary Layer Flow due to a Porous Rotating Disk with Heat Transfer*. Phys. Fluids, 21: 106104.
- TURKYILMAZOGLU M. 2012. *Solution of the Thomas-Fermi equation with a convergent approach*. Commun. Nonlinear Sci. Numer. Simul., 17: 4097–4103.
- TURKYILMAZOGLU M. 2013. *The analytical solution of mixed convection heat transfer and fluid flow of a MHD viscoelastic fluid over a permeable stretching surface*. Int. J. Mech. Sci., 77: 263–268.
- VARSHNEY C.L. 1979. *Fluctuating flow of viscous fluid through a porous medium bounded by a porous plate*. Indian J. Pure Appl. Math., 10(12): 1558–1564.
- WANG C.Y. 1988. *Nonlinear streaming due to the oscillatory stretching of a sheet in a Viscous fluid*. Acta Mech. 72: 261–268.
- ZHENG L., LIU Y., ZHANG X. 2011. *Exact solutions for MHD flow of generalized Oldroyd-B fluid due to an infinite accelerating plate*. Mathematical and Computer Modelling, 54: 780–788.
- ZHENG L.C., JIN X., ZHANG X.X., ZHANG J. H. 2013. *Unsteady heat and mass transfer in MHD flow over an oscillatory stretching surface with Soret and Dufour effects*. Acta Mechanica Sinica, 29(5): 667–675.